PHYSICAL REVIEW B **84**, 125202 (2011)

High-pressure study of the infrared active modes in wurtzite and rocksalt ZnO

J. Pellicer-Porres,[1,*] A. Segura,[1] V. Panchal,[1] A. Polian,[2] F. Decremps,[2] and P. Dumas[3]
[1]*MALTA Consolider Team, ICMUV, Universidad de Valencia, c/Dr. Moliner 50, E-46100 Burjassot, Valencia, Spain*
[2]*Institut de Minéralogie et de Physique des Milieux Condensés, CNRS-UMR 7590, Université Pierre et Marie Curie-Paris 6, B115, 4, Place Jussieu, F-75252 Paris CEDEX 05, France*
[3]*Synchrotron SOLEIL, L'Orme des Merisiers, Boîte Postale 48 Saint Aubin, F-91192 Gif-sur-Yvette Cedex, France*

(Received 4 May 2011; published 6 September 2011)

We present a high-pressure study of ZnO carried out in the mid- to far-infrared frequency domain with the aim of characterizing the optic modes of wurtzite and rocksalt ZnO. We obtained the pressure coefficients of the E_1(TO), E_1(LO), A_1(TO), and A_1(LO) modes of the low-pressure wurtzite phase and compare them with previous Raman measurements. The optical modes of the high-pressure rocksalt phase are infrared active, so we were able to determine their wave numbers and pressure dependencies. In the wurtzite phase, high pressure induces a slight decrease in both longitudinal and transverse effective charges. The decrease is more pronounced in the rocksalt phase.

DOI: 10.1103/PhysRevB.84.125202 PACS number(s): 78.30.Fs, 64.70.kg

I. INTRODUCTION

The present and potential applications of ZnO have attracted tremendous interest among the scientific community in recent years.[1,2] Restricted to optoelectronics, the interest in ZnO is stirred by the combination of the direct wide band gap (3.3 eV) and large exciton binding energy (60 meV). ZnO also has a simple crystal-growth technology, resulting in potentially low-cost ZnO-based devices.

A complete description of device performance requires a deep understanding of the thermal as well as electrical properties, which in turn heavily rely on the knowledge of their vibrational mode behavior. In this paper, we aim at investigating in depth the phonon mode behaviors under high pressure.

ZnO crystallizes in the wurtzite structure in ambient conditions. Under high pressure, it adopts the rocksalt structure. The phase transition presents a considerable hysteresis and is affected by the sample size and the pressure-temperature path followed.[3–6] At room temperature, the wurtzite to rocksalt phase transition is observed in bulk ZnO at 9 GPa whereas the reverse transition is detected in the downstroke at around 3 GPa. The effect of pressure in wurtzite lattice dynamics has been studied by Raman experiments under high pressure.[7–10] However, there is not a well-established consensus about the origin of the peaks observed at around 580 cm^{-1}, which has been assigned to the E_1(LO) mode,[8] the A_1(LO) mode,[9] or a combination of both modes.[10] Consequently, the characterization of the LO-TO splitting and its consequences in the evolution of the ionicity behavior in ZnO, expressed through the effective charge, are not clear. On the other hand, as the optical modes in the rocksalt phase are not Raman active and only Raman effect experiments have been carried out, there is a lack of experimental information about the LO and TO modes in this phase.

In this work, we have completed the study of wurtzite and rocksalt ZnO under high pressure using infrared (IR) microspectroscopy, thereby yielding the necessary complementary information to understand the lattice dynamics. We have characterized the optical modes in both polymorphs, deducing information about their pressure coefficients and characterizing the evolution of the ionicity through the effective charge.

II. EXPERIMENTAL METHODS

IR experiments under high pressure were performed with two different experimental setups. The first one is designed to measure the sample transmittance in the mid-infrared wavelength range. It was conducted on a commercially available Michelson Fourier-transform infrared (FTIR) spectrometer (TEO 400 FTIR Module by Science Tech), using the internal thermal source (globar) of this spectrometer. The exit port is made of KBr; from it a well-collimated and modulated infrared beam is extracted for the experiments. High pressure was generated with a membrane diamond anvil cell[11] (DAC) equipped with type-IIa diamond anvils with a culet diameter of 500 μm. The interfacing with the IR beam is based on a confocal horizontal all-reflective microscopic optical bench. The IR beam coming from the spectrometer first encounters a gold-coated 90° off-axis parabolic mirror, which converges the IR beam at one microiris, defining a variable slit to control the size of the IR beam in the sample chamber. Two reflecting gold-coated Cassegrain-type microscopic objectives (magnification 15×) are used to focus the beam on the sample. The IR beam from the second Cassegrain objective is spatially filtered by a pinhole and directed to an off-axis parabolic mirror, which focuses the IR beam on a mercury-cadmium-telluride detector. The pressure chamber is defined by a 250 μm hole drilled in an Inconel gasket. KBr was used as the pressure-transmitting medium. Pressure was measured with the ruby method.[12,13] The sample was pure ZnO either in powder form or as a single crystal. The single crystal had dimensions of about $110 \times 110 \times 25\ \mu\mathrm{m}^3$. The sample was cut with its bigger surface containing the c axis. A polarizer was used to select polarization parallel or perpendicular to the c axis. The transmittance was obtained by normalizing the spectrum measured through the sample with one reference spectrum previously measured through the empty DAC.

The second series of experiments was performed at the SMIS beamline[14] in the French National Synchrotron Facility

SOLEIL. We used a NicPlan IR microscope coupled to a FTIR spectrometer (Thermo Nicolet Magma 560). The microscope operated in confocal mode, using a 32× infinity-corrected Schwartzschild objective (numerical aperture 0.65) and a matching tenfold condenser. We used a Cu-Ge bolometer (Infrared Laboratories) cooled to liquid He temperature as a detector. The combination of detector, beam splitter, and filters established a useful spectral range between 100 and 600 cm^{-1}. The spectral resolution was set to 4 cm^{-1}. We accumulated 256 scans per spectrum. The high brilliance of the synchrotron radiation allows us to work with smaller samples (down to $\sim 15 \times 15\ \mu\text{m}^2$) than those of the setup with the globar source. In transmittance experiments, thanks to the small but bright synchrotron infrared beam, the reference beam was measured at each pressure through the diamonds in the void space next to the sample. In reflectance experiments, we took the reference spectrum using the metallic surface of the gasket as a mirror. The DAC loading conditions were very similar to those in the experiments performed in the mid-infrared, except that CsI was used as the pressure-transmitting medium instead of KBr.

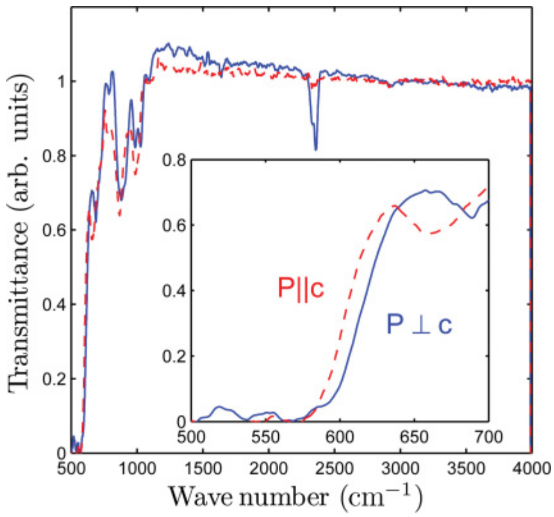

FIG. 2. (Color online) ZnO transmittance outside the DAC for two polarizations, parallel (dashed line) and perpendicular (continuous line) to the *c* axis.

III. RESULTS

A. Ambient pressure

The reflectance and transmission spectra at ambient pressure are represented in Figs. 1 and 2, respectively. The reflectance has been fitted with a single oscillator Lorentz model. The fit is represented in Fig. 1 with dashed lines. The corresponding physical parameters are summarized in Table I. We obtain in this way the wave number of the transverse optic mode (ω_{TO}), the static and high-frequency dielectric constants (ϵ_0 and ϵ_∞, respectively), and the damping parameter Γ. N is a normalization constant.

The experimental configuration limited the maximum useful wave number to 600 cm^{-1}. This restriction is the main reason for the uncertainty in the determination of the dielectric constant. In spite of that, our values are compatible with previous experiments available in the literature. The uncertainty does not affect the high-pressure characterization of the optical modes, which is the main objective of this work. Measurements in ambient conditions are only performed as a previous reference.

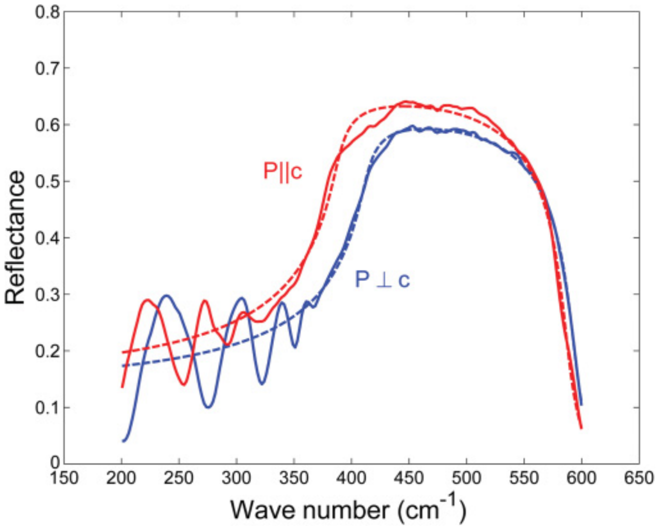

FIG. 1. (Color online) ZnO reflectance outside the DAC for two polarizations, parallel and perpendicular to the *c* axis. The experimental configuration limited the maximum useful wave number to 600 cm^{-1}. The dashed lines correspond to fits.

The wave numbers of the longitudinal optical modes have been deduced employing the Lyddane-Sachs-Teller relationship. Values are again in good agreement with previous measurements despite being affected by the cumulative uncertainty induced by error propagation.

B. High pressure

Figure 3 displays the ZnO reflectance as a function of high pressure. Recall that the spectral features over 600 cm^{-1} are related to noise due to the cutoff established by the bolometer filter. The incoming radiation was polarized in order to characterize both the A_1 ($P||c$) and E_1 ($P \perp c$) modes

TABLE I. Physical parameters obtained from a fit to the ZnO infrared spectra in ambient conditions for polarization P parallel and perpendicular to the c axis. ω_{TO}, ω_{LO}, and Γ are expressed in cm^{-1}.

	This work	Ref. 15	Ref. 16	Ref. 8	Ref. 17
			$P\|\|c$		
ϵ_0	8.7(6)		8.91(9)		
ϵ_∞	3.8(3)		3.78(5)		
$\omega_{\text{TO}}(A_1)$	389(2)	380		382	380
$\omega_{\text{LO}}(A_1)$	590(50)	570	577.1(4)	574	579
Γ	16(3)				
N	71(3)				
			$P \perp c$		
ϵ_0	8.2(9)		7.77(3)		
ϵ_∞	4.0(5)		3.70(1)		
$\omega_{\text{TO}}(E)$	413(4)	412	408.2(3)	414	413
$\omega_{\text{LO}}(E)$	590(50)	591	592.1(2)	580	591
Γ	16(5)				
N	67(3)				

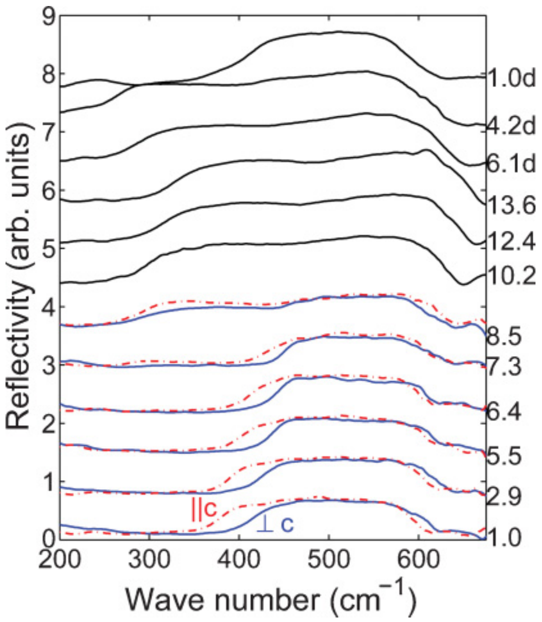

FIG. 3. (Color online) High-pressure evolution of the reflectance measured with a ZnO single crystal. Numbers next to the spectra indicate the pressure in GPa. Spectra measured in the downstroke are labeled with an additional *d*. In the low pressure phase, we selected polarization *P* parallel and perpendicular to the *c* axis. From 10.2 GPa to the maximum pressure and also at the downstroke, we performed unpolarized measurements.

of the wurtzite phase. From ambient pressure to 7.3 GPa a continuous shift of the spectra is observed. At 7.3 GPa there is a small but clear increase in intensity around 300 cm^{-1}, indicating the beginning of the phase transition to the rocksalt phase. At 8.5 GPa we observe a phase mixture with a wider reststrahlen region but with anisotropy still present. At 10.2 GPa the spectrum of the rocksalt phase did not show any dichroism, and the spectra were measured without polarizing the infrared radiation. The rocksalt phase is maintained in the downstroke down to 1 GPa where there are again signs of phase mixture.

The high-pressure dependence of the A_1(TO) and E_1(TO) wave numbers of the wurtzite phase, as well as the evolution of the TO mode of the rocksalt phase, have been determined by the pressure shift of the spectra, following a constant-intensity point of the spectra. In this way we have access to the evolution of the phonon wave number with respect to the ambient-pressure spectra. The absolute values have been calibrated from the results presented in Table I. The pressure evolution of the phonon wave numbers is shown in Fig. 4.

Complementary information has been extracted from high-pressure transmission experiments. We show in Fig. 5 the transmittance of a ZnO single crystal. The phase transition sequence is in perfect agreement with the previous experiment, showing subtle modifications at the very beginning of the phase transition at 7.4 GPa, clear changes at 8.7 GPa, and a nearly completed phase transition at 10.1 GPa.

The wave number changes of the A_1(LO) and E_1(LO) modes of the wurtzite phase have also been determined by the shift of constant-intensity points as explicitly shown in Fig. 5. At the highest pressure, the sample was stacked by the gasket, so data measured in the downstroke were not reliable. We characterized the LO mode of the ZnO rocksalt phase with an additional experiment carried out with a powdered sample. In this case we faced interference features which obscured the spectra in the upstroke. When pressure was released, the pressure chamber thickness did not change as much as in the upstroke, and the interference pattern remained stable, allowing us to characterize the rocksalt LO mode. The spectra displayed in Fig. 6 were thus measured in the downstroke.

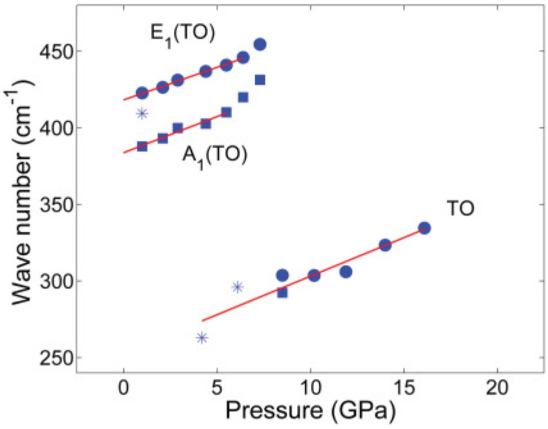

FIG. 4. (Color online) Pressure dependence of TO phonon wave numbers. Circles (squares) represent wave numbers determined with the polarization oriented perpendicular (parallel) to the *c* axis of a single crystal. Stars correspond to the downstroke data measured with unpolarized light.

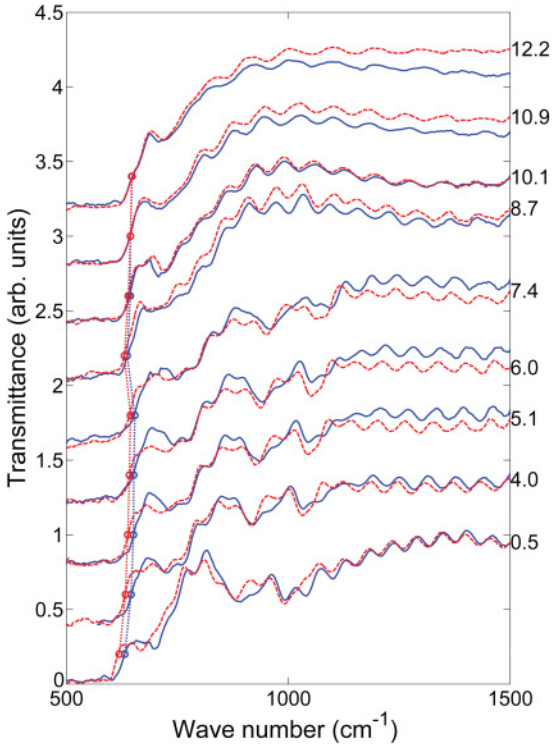

FIG. 5. (Color online) ZnO single crystal transmittance under high pressure. The polarization was either parallel (dashed line) or perpendicular to the *c* axis. Numbers next to the spectra indicate the pressure in GPa. Circles indicate constant intensity points.

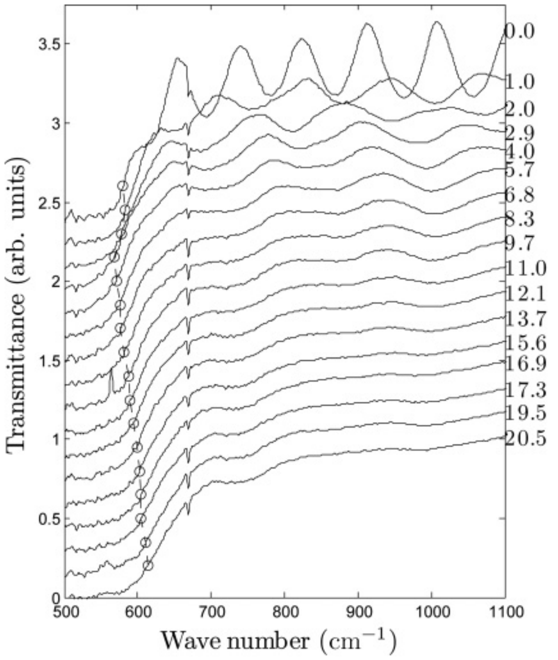

FIG. 6. ZnO transmittance spectra of a powdered sample. All the spectra have been measured in the downstroke. Circles indicate constant intensity points.

The pressure dependence of the phonon rocksalt LO mode is presented in Fig. 7 with stars.

IV. DISCUSSION

A. Wurtzite phase

The pressure dependence of transverse optical modes is presented in Fig. 4. In the upstroke, the single-crystal experiment allowed us to characterize the pressure evolution of both the E_1(TO) and A_1(TO) modes. The pressure coefficients are summarized in Table II, which demonstrates the perfect agreement with our previous Raman experiments.[8] The pressure shift of the A_1(TO) mode is larger than that of the E_1(TO) mode. As the phase transition to the rocksalt phase takes place, the wave numbers of both modes converge to the rocksalt phase TO wave number. In the downstroke, the rocksalt phase is maintained down to 2.5 ± 1.5 GPa. The recovered wurtzite phase is no longer single crystalline, and consequently only the A_1(TO) mode can be characterized in the downstroke.

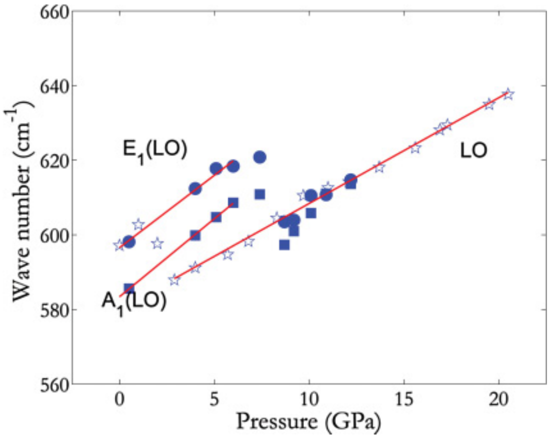

FIG. 7. (Color online) Pressure dependence of LO phonon wave numbers. Circles (squares) represent wave numbers determined with the polarization oriented perpendicular (parallel) to the c axis of a single crystal. Stars correspond to the downstroke data measured with unpolarized light and a powdered sample.

TABLE II. Pressure coefficients of infrared active modes in wurtzite ZnO, expressed in cm^{-1}/GPa.

	This work IR	Ref. 8 Raman	Ref. 10 Raman	Ref. 9 Raman
E_1(LO)	3.9(4)	4.78	4.55(10)	
A_1(LO)	4.2(2)		4.56(7)	4.75(9)
E_1(TO)	4.3(4)	4.38	5.03(3)	5.2(2)
A_1(TO)	4.7(5)	4.72	4.91(5)	4.33(8)

The overall behavior of the longitudinal optical modes (see Fig. 4 and Table II) is very similar to that of the transverse optical modes just discussed. A significant discrepancy between the pressure coefficients determined with our infrared experiment for the E_1(LO) and A_1(LO) modes with respect to those coefficients measured in Raman experiments (including our previous ones) is evident. One reason that could be argued to explain this discrepancy is the different pressure-transmitting media employed in infrared (KBr) and Raman (Ne) experiments. However, the agreement observed in the pressure coefficients of the transverse optical modes disallows this hypothesis. Let us focus now on the experimental conditions of Raman experiments. Most high-pressure investigations are carried out in the backscattering configuration. In this configuration, the observation of the E_1(LO) mode is forbidden by selection rules. In Ref. 8, experiments were performed with incident radiation along the c axis. The vibration with A_1(LO) symmetry, although allowed, is very weak[19] and was not observed inside the diamond anvil cell. The E_1(LO) mode was observed only when the excitation laser was focused on the sample border. Under these conditions the scattering configuration is not well defined. Consequently, the E_1(LO) symmetry assignment was qualified as tentative. In Ref. 9, an asymmetric structure appearing at 576 cm^{-1} was only observed in the downstroke after backtransformation to the wurtzite structure and was assigned to the A_1(LO) mode. The low-energy component of the asymmetric peak was attributed to disorder-induced scattering of LO phonons from the border of the Brillouin zone. With respect to the experiment described in Ref. 10, the excitation laser radiation propagated along a direction perpendicular to the c axis. Neither the A_1(LO) mode nor the E_1(LO) mode is allowed. According to the authors, they were observed due to the large numeric aperture of the focusing objective. The spectral feature corresponding to both modes, located around 582 cm^{-1}, consisted of a broad peak that was separated into two components after a fitting procedure. We conclude then that, in the three experiments reported, the scattering configuration was not appropriate for unambiguously characterizing the pressure behavior of the longitudinal optical modes.

The TO-LO splitting has been used in previous works on ZnO to obtain information about the evolution of the polar character of the Zn-O bond under high pressure through the effective charge e^* appearing in the equation[20]

$$(e^*)^2 = 4\pi^2 V \mu \epsilon_0 \epsilon_\infty \left(\nu_{\mathrm{LO}}^2 - \nu_{\mathrm{TO}}^2\right), \quad (1)$$

where V is the volume per formula unit, μ is the reduced mass, ϵ_0 is the vacuum permittivity, and ϵ_∞ is the high-frequency (optical) dielectric constant. Pressure induces changes in V, ϵ_∞, and phonon frequencies. The effect of pressure on V is given by the equation of state. We used the bulk modulus (173 GPa) determined by x-ray diffraction in Ref. 6. The pressure dependence of ϵ_∞ has not been measured. As an approximation, in Refs. 10 and 8 its magnitude was deduced from the dependence of the refractive index measured by Vedam *et al.*[21] at 589.3 nm, assuming that $\frac{\partial \epsilon_\infty}{\partial P} \simeq 2n\frac{\partial n}{\partial P}$. We employ the same approximation. Finally, the pressure coefficients of the phonon modes established in this work can be used to calculate the effective charge evolution under high pressure. It should be noted that the contribution of the phonon modes to the sign of $\frac{\partial e^*}{\partial P}$ is not only due to the increase or decrease of the LO-TO splitting, but because $\nu_{\mathrm{LO}}^2 - \nu_{\mathrm{TO}}^2 = (\nu_{\mathrm{LO}} - \nu_{\mathrm{TO}})(\nu_{\mathrm{LO}} + \nu_{\mathrm{TO}})$, the pressure coefficients of the modes themselves play a fundamental role. In particular, $\nu_{\mathrm{LO}}^2 - \nu_{\mathrm{TO}}^2$ can increase even if $\nu_{\mathrm{LO}} - \nu_{\mathrm{TO}}$ decreases.

The results concerning the effective charge are summarized in Table IV. The considerable uncertainties quoted in the table come on the one hand from the rough approximation used to estimate $\frac{\partial \epsilon_\infty}{\partial P}$ and on the other hand from the determination of the E_1 and A_1 pressure coefficients. We obtained a slight diminution of the effective charge under high pressure in contrast with the increments found in Refs. 8 and 9 where, notwithstanding that, the uncertainties associated with the derivation of the effective charge suggest that the results indicated a small variation of the wurtzite Zn–O ionicity under high pressure. The decrease deduced from our IR experiment is not as pronounced as the one found in Ref. 10. The main source of discrepancy is related to the differences in phonon pressure coefficients already explained in the preceding section. Finally, our results are in agreement with the *ab initio* calculations performed in Ref. 18. We then conclude again that the bond ionicity is slowly varying in wurtzite ZnO under high pressure.

TABLE IV. Pressure evolution of effective charge in wurtzite and rocksalt ZnO. The effective charge is written in terms of the fundamental electronic charge. $\partial e^*/\partial P$ is in 10^{-3} GPa units.

	This work IR	Ref. 8 Raman	Ref. 9 Raman	Ref. 10 Raman	Ref. 18 Calculated
		Wurtzite			
$\partial e^*_\perp/\partial P$	$-4(2)$	6.4		$-6.3(2)$	-3.0
$\partial e^*_\parallel/\partial P$	$-3(2)$		1.5(8)	$-6.7(2)$	-2.8
		Rocksalt			
$\partial e^*/\partial P$	$-8(2)$				-2.2

B. Rocksalt phase

The rocksalt phase has no Raman active modes, so this work constitutes, to the best of our knowledge, the first experimental study of rocksalt lattice vibrations. We report in Table III the phonon wave numbers and pressure coefficients of the LO and TO modes. The TO wave number obtained is compatible with results of *ab initio* calculations,[18] but the experimental LO-TO splitting was found to be 10% larger than the calculated one. With respect to other rocksalt II-VI oxides,[22] rocksalt ZnO TO and LO wave numbers are comparable to those of CdO (262 cm and 528 cm^{-1}) and CaO (293 and 547 cm^{-1}) and are smaller than those of the lighter MgO (402 and 717 cm^{-1}).

The effective charge analysis performed with the wurtzite phase can be recalculated for the rocksalt polymorph. The rocksalt phase is less compressible, with a 204 GPa bulk modulus.[6] The high-frequency dielectric constant of the rocksalt phase has been estimated[23] from the plasma frequency of Ga-doped ZnO, obtaining $\epsilon_\infty = 3.4 \pm 0.3$. With respect to its pressure variation and due to the lack of experimental data, we must consider the calculated[18] variation of the high-frequency dielectric constant, $\frac{\partial \epsilon_\infty}{\partial P} = -0.017$ GPa^{-1}. With all these data, Eq. (1) results in $e^* = 2.2$ with a decrease under high pressure given by $\frac{\partial e^*}{\partial P} = -0.008(2)$ GPa^{-1}. Before comparison with the calculation, we must take into account that the ϵ_∞ obtained from the *ab initio* calculation,[18] $\epsilon_\infty = 5.4$, is overestimated. This is related to the inherent problems of the local density approximation in describing excited states and consequently in yielding correct values for electronic transitions. The high-frequency dielectric constant is related to the Penn gap (E_{Penn}) by $\epsilon_\infty - 1 = \frac{E_p^2}{E_{\mathrm{Penn}}^2}$, where E_p is the plasma energy. A too small Penn gap is then reflected in an overestimation of ϵ_∞. The value of the effective charge pressure coefficient given in Ref. 18 (see Table IV) can be recalculated using the experimental ϵ_∞, resulting (at 10 GPa) in -0.004 GPa^{-1}. Experiments and calculations agree then in signaling a greater diminution of the bond ionicity in the rocksalt phase than in the wurtzite phase.

TABLE III. Pressure evolution of infrared active modes in rocksalt ZnO. Wave number is expressed in cm^{-1} and pressure in GPa.

	This work IR	Ref. 18 Calculated
LO	$580(20) + 2.8(1)P$	$528 + 3.68P - 0.028P^2$
TO	$250(20) + 5.0(5)P$	$235 + 5.14P - 0.053P^2$

V. CONCLUSIONS

We have performed a set of optical experiments in the mid- and far-infrared region on ZnO under high pressure. The LO modes have been characterized in a laboratory setup with a globar source whereas the TO modes have been followed under high pressure in a synchrotron infrared beamline. We have used single crystals and polarized radiation in order to distinguish between the wurtzite A_1 and E_1 modes. The phonon pressure dependence is summarized in Table II. High pressure induces a decrease of the LO-TO splitting, resulting in a small reduction of ionicity as deduced from the pressure coefficients of both the transverse and longitudinal effective charges (Table IV). This work also reveals additional behavior of the optical modes in rocksalt ZnO (Table III). In this polymorph, the rate at which the ionicity decreases is larger than in wurtzite ZnO.

ACKNOWLEDGMENTS

We acknowledge the Ministerio de Ciencia y Tecnología of Spain (Projects No. MAT2008-06873-C02-02 and No. MAT2010-21270-C04-01 and MALTA Consolider Initiative No. CSD2007-00045). We thank the managers of SOLEIL Synchrotron for granting us beam time.

---

[*] julio.pellicer@uv.es

[1] S. J. Pearton, D. P. Norton, K. Ip, Y. W. Heo, and T. Steiner, Prog. Mater. Sci. **50**, 293 (2005).

[2] U. Ozgur, Y. I. Alivov, C. Liu, A. Teke, M. A. Reshchikov, S. Dogan, V. Avrutin, S.-J. Cho, and H. Morkoc, J. Appl. Phys. **98**, 041301 (2005).

[3] S. Desgreniers, Phys. Rev. B **58**, 14102 (1998).

[4] F. Decremps, J. Zhang, and R. Liebermann, Europhys. Lett. **51**, 268 (2000).

[5] F. Decremps, J. Pellicer-Porres, F. Datchi, J. P. Itié, A. Polian, F. Baudelet, and J. Z. Jiang, Appl. Phys. Lett. **81**, 4820 (2002).

[6] F. Decremps, F. Datchi, A. M. Saitta, A. Polian, S. Pascarelli, A. Di Cicco, J. P. Itié, and F. Baudelet, Phys. Rev. B **68**, 104101 (2003).

[7] S. S. Mitra, O. Brafman, W. B. Daniels, and R. K. Crawford, Phys. Rev. **186**, 942 (1969).

[8] F. Decremps, J. Pellicer-Porres, A. M. Saitta, J.-C. Chervin, and A. Polian, Phys. Rev. B **65**, 092101 (2002).

[9] F. J. Manjón, K. Syassen, and R. Lauck, High Press. Res. **22**, 299 (2002).

[10] J. S. Reparaz, L. R. Muniz, M. R. Wagner, A. R. Goni, M. I. Alonso, A. Hoffmann, and B. K. Meyer, Appl. Phys. Lett. **96**, 231906 (2010).

[11] R. LeToullec, J. Pinceaux, and P. Loubeyre, High Press. Res. **1**, 77 (1988).

[12] J. C. Chervin, B. Canny, and M. Mancinelli, High Press. Res. **21**, 305 (2001).

[13] H. Mao, J. Xu, and P. Bell, J. Geophys. Res. **91**, 4673 (1986).

[14] P. Dumas, F. Polack, B. Lagarde, O. Chubar, J. L. Giorgetta, and S. Lefrancois, Infrared Phys. Technol. **49**, 152 (2006).

[15] E. F. Venger, A. V. Melnichuk, L. Y. Melnichuk, and Y. A. Pasechnik, Phys. Status Solidi B **188**, 823 (1995).

[16] N. Ashkenov, B. N. Mbenkum, C. Bundesmann, V. Riede, M. Lorenz, D. Spemann, E. M. Kaidashev, A. Kasic, M. Schubert, M. Grundmann, G. Wagner, H. Neumann, V. Darakchieva, H. Arwin, and B. Monemar, J. Appl. Phys. **93**, 126 (2003).

[17] C. A. Arguello, D. L. Rousseau, and S. P. S. Porto, Phys. Rev. **181**, 1351 (1969).

[18] J. Serrano, A. H. Romero, F. J. Manjón, R. Lauck, M. Cardona, and A. Rubio, Phys. Rev. B **69**, 094306 (2004).

[19] R. Cuscó, E. Alarcón-Lladó, J. Ibáñez, L. Artús, J. Jiménez, B. Wang, and M. J. Callahan, Phys. Rev. B **75**, 165202 (2007).

[20] M. Fox, *Optical Properties of Solids* (Oxford University Press, Oxford, 2001).

[21] K. Vedam and T. A. Davis, Phys. Rev. **181**, 1196 (1969).

[22] O. Madelung, *Semiconductors: Data Handbook* (Springer-Verlag, Berlin, 2004).

[23] A. Segura, J. A. Sans, D. Errandonea, D. Martinez-Garcia, and V. Fages, Appl. Phys. Lett. **88**, 011910 (2006).